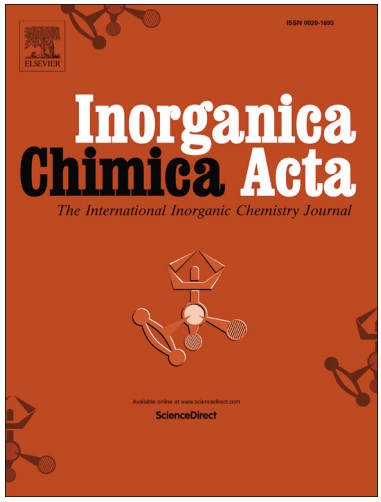

Platinum(II)-Glutamic Acid Dendrimer Conjugates: Synthesis, Characterization, DFT Calculation, Conformational Analysis and Catalytic Properties

Anas Lataifeh, Heinz-Bernhard Kraatz, Firas F. Awwadi, Mohammed A. Zaitoun, Ken Sakai

PII: S0020-1693(17)31692-4
DOI: https://doi.org/10.1016/j.ica.2017.12.022
Reference: ICA 18056

To appear in: *Inorganica Chimica Acta*

Received Date: 5 November 2017
Revised Date: 11 December 2017
Accepted Date: 14 December 2017

Please cite this article as: A. Lataifeh, H-B. Kraatz, F.F. Awwadi, M.A. Zaitoun, K. Sakai, Platinum(II)-Glutamic Acid Dendrimer Conjugates: Synthesis, Characterization, DFT Calculation, Conformational Analysis and Catalytic Properties, *Inorganica Chimica Acta* (2017), doi: https://doi.org/10.1016/j.ica.2017.12.022

Platinum(II)-Glutamic Acid Dendrimer Conjugates: Synthesis, Characterization, DFT Calculation, Conformational Analysis and Catalytic Properties

Anas Lataifeh,*[a] Heinz-Bernhard Kraatz,[b] Firas F. Awwadi,[c] Mohammed A. Zaitoun[d] and Ken Sakai[e,f,J]

[a] *Tafila Technical University*, *Department of Chemistry*
Tafila 66110, JORDAN
Phone: *962 079 730 1239*, E-mail: *lataifeh@ttu.edu.jo*

[b] *University of Toronto at Scarborough*, *Department of Physical and Environmental Sciences*
1265 Military Trail, *Toronto*, *Ontario*, CANADA
Phone: *1 416 287 7278*, E-mail: *bernie.kraatz@utoronto.ca*

[c] *The University of Jordan*, *Department of Chemistry*
Amman 11942, JORDAN
Phone: *962 0798137584,* E-mail: *f.awwadi@ju.edu.jo*

[d] *Mutah University*, *Department of Chemistry*
Karak, JORDAN
Phone: *962 779692326,* E-mail: *zaitoun444@yahoo.com*

[e] *Kyushu University, Department of Chemistry*
Hakozaki, *Higashi-Ku*, *Fukuoka 812-858*, JAPAN
Phone: *81 92 642 2596*, E-mail: *ksakai@chem.kyushu-univ.jp*

[f] *Kyushu University, International Institute for Carbon Neutral Energy Research (WPI-I2CNER)*
744 Moto-oka, *Nishi-ku*, *Fukuoka 819-0395*, JAPAN

[J] *Kyushu University, International Research Center for Molecular Systems (IRCMS)*
744 Moto-oka, *Nishi-ku*, *Fukuoka 812-858*, JAPAN

Keywords: Bioinorganic / Homogeneous catalysis / Complexes / Platinum / Dendrimers / Hydrogen evolution

Abstract

A series of platinum(II)-*L*-glutamic acid dendrimer conjugates having the formula $PtCl_2$(5,5'-Gn(OR)-2,2'-bipyridine); Gn (n = 0, 1, 2), have been synthesized by various amide bond formation methods. The dendrimer complexes were terminated as carboxylic acid (R = H) or methyloxy ester (R = Me). The complexes were characterized by mass spectrometry, elemental analysis, UV-vis, FTIR, ^{1}H-, ^{13}C-NMR, ^{1}H-TOCSY, HSQC. The G1(OH) complex aggregate in solution and solid state, giving rise to a rigid conformation for the glutmaic acid side chain. The G2(OH) exists in the "monomeric" form with several conformations for the glutamic acid side chains. Complexes terminated with carboxyl group (R = H) were active catalyst toward hydrogen gas (H_2) production by photo-induced splitting of water. The turnover frequency (TOF) for the G1(OH) (14.7×10^{15} s^{-1}) exhibited a ~2-fold enhancement in H_2 production compared to the unmodified parent catalyst G0(OH) (TOF = 7×10^{15} s^{-1}). While G2(OH) displayed a lower hydrogen activity (TOF = 3.8×10^{15} s^{-1}) compared to G0(OH). The platinum-glutamic acid dendrimer conjugates showed a correlation between H_2 evolution activity and their ability to form aggregates, which driven by the steric hindrance of the peptide residues in the vicinity of Pt-center.

Introduction

The Chemistry of platinum(II) complexes have attracted considerable attention for many years in part due to their applications in the fields of organic light emitting devices (OLEDs),[1] cancer therapy,[2, 3] and catalytic processes.[4, 5] Most of the reported studies on platinum(II)-peptide conjugates were examined for their antitumor activity,[2, 6] and only few examples have discussed their catalytic properties.[7, 8] To rationalize some of the functional and structural properties of naturally occurring redox metalloproteins,[9, 10] amino-acid conjugates containing redox active transition metal center (e.g. Ni, Co) have been exploited.[11, 12] In these studies the peptide scaffolds were based on non-natural amino acids, moreover, the exact peptide structure around the active core is quite unknown. The latter issue is of special interest due to the fact that the amino acids, which lie in close proximity to the active site of metalloproteins, play key role in regulating and enhancing enzyme activity.[13] Accordingly, and for all of the above examples and limitations, we were motivated to synthesize a series of new platinum(II)-centered peptide dendrimer conjugates and to study their catalytic activities toward photoinduced hydrogen evolution from water. The Pt-peptide conjugate structure-activity relationship has been addresed.

Among various reported molecular catalysts for hydrogen evolution from water,[12, 14-17] platinum(II)-based molecular catalysts were quite unique due to their applicability as catalysts for a well-known photo-system consisting of tris(2,2'-bipyridine)ruthenium(II) ($[Ru(bpy)_3]^{2+}$), methylviologen (MV^{2+}, *N*,*N*'-dimethyl-4,4'-bipyridinum) cation and ethylenediaminetetracetic acid disodium salt (Na_2EDTA).[16] The hydrogen evolution from water in such system proceeded as a dark reaction in the presence of platinum(II)-based molecular catalysts.[16] Furthermore, mechanistic studies revealed that hydrogen evolution reaction is likely to proceed *via* the formation of hydridoplatinum(III) intermediate ($Pt(II) + H^+ + e^- \rightarrow Pt(III)\text{-}H$).[18] In these studies, the $PtCl_2(bpy)$ complex, bpy = 2,2'-bipyridine, has been often employed as an H_2-evolving center.

Peptide dendrons based on natural *L*-glutamic acid are well known in literature.[19] The dendron size (peptide layers), dendron structure (open *vs*. backfolded) and surface functionality were controllable. The *L*-glutamic acid dendron conjugates to ferrocene and Pd-porphyrin core were reported.[20, 21] The electron and substrate transfer properties in *L*-glutamic acid dendron were realized. Therefore, the coupling of *L*-glutamic acid peptide dendrons to $PtCl_2(bpy)$ complex generate a synthetic molecular model, in which the peptide environment arround the H_2-production center mimics those in metalloproteins.

Herein, we report the detailed synthetic procedures, physical properties and conformational analysis of new platinum(II)-*L*-glutamic acid dendrimer conjugates having the general formula [$PtCl_2$(5,5'-Gn(OR)-2,2'-bpy)], n (generation number) = 0, 1, 2; R = H (peripheral group = carboxylic acid), R = Me (peripheral group = methoxyester), Figure 1a. The catalytic activity of $PtCl_2$(5,5'-Gn(OR)-

2,2'-bpy) peptide conjugates toward hydrogen evolution from water was correlated to the peptide dendrimer structure adopted by each dendrimer generation, Figure 1b.

Methods and Materials

Experimental Section

General Remarks: H_2N-Glu(OMe)-OMe·HCl,[22] and Boc-Glu(OH)-OH,[23] were prepared by a modified procedure from H_2N-Glu(OH)-OH (Aldrich), thionyl chloride ($SOCl_2$) (Alfa Aesar) and di-tert-butyl dicarbonate (Boc_2O) (Advanced ChemTech), respectively. 1-ethyl-3-(3-dimethylaminopropyl)carbodimide hydrochloride (EDC·HCl) and 1-hydroxybenzotriazole monohydrate (HOBt·H_2O), ethylenediaminetetracetic acid disodium salt (EDTA), dimethylsulfoxide (DMSO) and 5,5•-dimethyl-2,2•-bipyridine were obtained from Advanced ChemTech. *cis*-$PtCl_2(DMSO)_2$, $[MV](NO_3)_2$ and $[Ru(bpy)_3](NO_3)_2 \cdot 3H_2O$ were prepared as previously described.[24] The K_2PtCl_4 was received from Tanka Kikinzaku Kogyo. All other reagents were purchased in their highest quality available. Pure water of high resistivity (18.2 MΩ) was obtained by Millipore water system (Millipore Corporation). All syntheses were carried out in air unless otherwise stated. Deuterated chloroform ($CDCl_3$) (Sigma-Aldrich) was stored over molecular sieves (8–12 mesh; 4Å effective pore size; Fisher) under inert atmosphere. Deuterated [D6] DMSO ampoule (1 mL) obtained from Sigma-Aldrich.

Instrumentation and Methods: The mass spectrometry measurements were carried out on Finnigan MAT 8400 and Bruker Apex IV time-of-flight mass spectrometry (TOF-MS). UV–Vis and VT-UV-vis measurements were recorded using Shimadzu (UV-1800) spectrophotometer. The VT-UV-vis measurments were performed in 5 mM aqueous NaCl solution.

The NMR spectra were recorded on a Varian INOVA 600 MHz spectrometer using a 5 mm z-gradient triple resonance inverse HCX probe, operating at 600.23 MHz (^{1}H) and 150.78 MHz (^{13}C) at 24 ± 1 ºC. The ^{1}H NMR spectra were recorded with a 45º pulse angle, spectral width 9590 Hz and 128 scans. The data were reported as follows: the chemical shifts were referenced to the residual in $CDCl_3$ and [D6] DMSO on the δ scale (ppm), integration, multiplicity (s, singlet; d, doublet; ddd, douplet of douplet of douplets; t, triplet and m, multiplet), coupling constants (Hz) and 2D TOCSY (Total Correlation Spectroscopy). The TOCSY spectra were obtained with 2 scans for each 200 t1 increments. A spectral width of 9593.5 Hz was used in both dimensions with mixing time of 80 ms and a relaxation delay of 1.0 s. Zero filling was applied to give a final matrix of 1×1 K. ^{13}C NMR spectra were recorded with a 90º pulse angle, 2s relaxation delay and a spectral width 9590 Hz. Chemical shifts were in on the δ scale (ppm) and referenced to the residues present

in $CDCl_3$ and [D6] DMSO. Gradiant phase 2D HSQC experiments were performed with 2 scans for each of 256 t1 increments and relxation delay of of 1.0s. The ^{1}H spectral width was 9590 Hz and the ^{13}C spectral width was 31658.1 Hz. The NMR experimens of the Pt-complrxes (in DMSO) were carried out within very short period of time after the NMR solution mixture had been made, this to avoid any possible hydrolysis of the chlorido ligands

Fourier transform infrared spectroscopy (FTIR) spectra were recorded on Nicolet Impact 400 FTIR spectrophotometer (Nicolet Analytical Instrument) using KBr pellets at 2.0 cm^{-1} resolution. The IR results were reported as: s, strong; bar, broad; w, week. Melting point measurements were recorded using Brenstated Electrothermal apparatus. Photoluminesence data were obtained under the continuous Xe lamp (150 W) excitation in a John Yvon Fluoromax P spectrofluorometer at room temperature for the acid terminated Pt-complexes: **1**, **5**, **7**.

Elemental analysis was carried out on a Leeco CHNS-932 Elemental Analyzer at the institute of organic chemistry and macromolecular chemistry, Friedrich Schiller-University of Jena. Elemental analyses have been carried out only for Pt-complexes: **1**, **4**, **5**, **6**, **7**.

DFT calculation: The molecular structures of the conjugates were optimized at DFT/B3LYP level using Gaussian 09 package.[25] cc-pvdz basis sets are assigned to C, H, N, and Cl and LANL2DZ to Pt. The UV-Vis spectra of **1** and **5** and their molecular orbital analysis were carried out using Gaussian 09 and GaussSum 3 programs.[26] Time dependent density TD-DFT was used to calculate the UV-Vis spectra in water. Conductor-like Polarizable Continuum Model (CPCM) was used as solvation model.

Hydrogen evolution study: Photochemical hydrogen production from water was analyzed by using an automatic H_2 monitoring system. In this system, continuous flow of Ar (10.0 ml/min, controlled by a STEC SEC-E40/PAC-D2 digital mass flow controller) was bubbled through a photolysis solution (10 ml) contained in a cylindrical shaped, Pyrex glass vial (30 ml). The vent gas from the vial was introduced into a 6-way valve which allowed the automatic injection of the sample gas onto a gas chromatograph (Shimadzu GC-14A equipped with a Molecular Sieve 5A column of 2 m x 3 mm I.D., and thermostated at 30 ºC).

The injection of the sample gas and the output signal from the thermal conductivity detector of the gas chromatograph were both controlled by the a control software. Photolysis solutions were stirred continuously and irradiated after deaerateding with Ar for at least 30 min prior to the photolysis. The photoirradiation was carried out by an Ushio xenon short arc lamp UXL500D-O (operated at 350 W, $550 > \lambda > 240$ nm). Photolysis vial was immersed in a water bath thermostated at 20 ºC to remove IR radiation and to eliminate the temperature effect. The optical path between the photolysis solution and the Xe lamp were always given by Pyrex glass.

The photolysis solution contains aqueous acetate buffer (30 mM CH_3COOH/70 mM CH_3COONa, pH = 5.0, 10 mL) containing 30 mM EDTA, 0.04 mM $[Ru(bpy)_3](NO_3)_2 \cdot 3H_2O$, 2 mM $[MV](NO_3)_2$ and 100 mM NaCl in the presence of either **1** (0.5530 mg), **5** (0.8140 mg) or **7** (1.3070 mg) at a concentration of 0.1 mM. Sodium chloride salt was added to preclude hydrolysis of chlorido ligands in complexes **1**, **5** and **7**.[28] . The initial very short induction period (*ca.* 5 min) is consistent with the time required to obtain a blue photolysis solution, at the end of which the $MV^{\cdot+}$ concentration is maximized. The photolysis was carried out under argon atmosphere for ~ 5 hr. The calculation of the turnover frequency (TOF, H_2 molecule/sec) was based on the total number of hydrogen gas molecules produced over 5 hours.

Syntheses:

Synthesis of 2,2′-bpy-5,5′-dicarboxylic acid (dcbpy) ligand:[24] A suspension of 5,5′-dimethyl-2,2′-bpy (1.51 g, 8.2 mmol) was dissolved in 100 mL water. Solid $KMnO_4$ (8.57 g, 54.2 mmol) was added to the initial suspension. Then, the reaction mixture was stirred and heated up to 80–85 ºC for 24 h. The deep black solution was cooled to r.t. and filtered off using frit funnel; the aqueous phase was then neutralized with concentrated HCl, resulting in the formation of white suspension. The solid was then filtered under vacuum. The white powder was collected and dried in vacuum desiccators. Yield: 1.33 g, 54 %. ^{1}H NMR (600 MHz, [D6] DMSO): δ = 9.29 (s, 2H, 6,6'-bpy), 8.57 (m, 2H, 3,3'-bpy), 8.45 (m, 2H, 4,4'-bpy).

Synthesis of $Pt(dcbpy)Cl_2$ (**1**):[24] The *cis*-$PtCl_2(DMSO)_2$ (0.1060 g, 0.25 mmol) was dissolved in methanol (20 mL) followed by addition of solid 5,5'-dicarboxylic acid-2,2'-bpy (dcbpy) (0.0490 g, 0.20 mmol). The resultant suspension was sealed in a pressure-resistant vial and reacted at 120 °C for 6 h. Upon cooling the vial, bright yellowish-orange crystals were formed. The crystals were filtered off and washed several times with cold acetone. To remove trace impurities, the product was purified by recrystallization from hot ethanol/water mixture. The collected crystals were dried in a vacuum desiccator. Yield: 0.04, 44%. M.p. = 383 °C (decomp.). TOF MS ESI$^-$ (1:1 (v/v), CH_3OH, H_2O): *m/z* = 508.9715 $[M–H]^{-1}$ calc. for $C_{12}H_7N_4O_4PtCl_2$ requires 509.1789. IR (KBr, cm^{-1}): 3055 (br, O–H), 1700 (s, CO_{acid}), 1605 (s, $C{=}C_{aromatic}$), 1290 (s, C–O). ^{1}H NMR (600 MHz, [D6] DMSO): δ = 9.99 (s, 2H, 6,6'-bpy), 8.80 (m, 2H, 4,4'-bpy), 8.78 (m, 2H, 3,3'-bpy). ^{13}C NMR (150.78 MHz, DMSO-d_6): δ = 166.2 (CO_{acid}), 157.6 ($C_{6,6'}$), 150.6 ($C_{2,2'}$), 138.9 ($C_{5,5'}$), 127.5 ($C_{4,4'}$), 121.5 ($C_{3,3'}$). UV-vis (H_2O, λ_{max} (nm): 258 (C=O), 318, 333 (bpy), 370 (MLCT). Anal. Calcd.for $C_{12}H_8Cl_2N_2O_4Pt$: C 28.25, H 1.58, N 5.49; found C 28.02, H 1.51, N 5.39.

Synthesis of 5,5′-bis(chlorocarbonyl)-2,2′-bpy:[24] A suspension of 2,2′-bpy-5,5′-dicarboxylic acid (3.50 g, 11.6 mmol) in $SOCl_2$ (9.0 mL, 124.0 mmol) was stirred at r.t. under Ar atmosphere. 1-2

drops of *N*,*N*′-dimethylformaide (DMF) was added to enhance solubility of the dcbpy ligand. The reaction was heated up to 40 ºC. After several hours, chunks of dcbpy were still insoluble in $SOCl_2$. To ensure complete solubility, a 10 mL of tetrahydrofuran (THF) was added. The heating was continued for a total of 6 hr. The solution was cooled down to r.t. and the excess $SOCl_2$ was removed by rotary evaporator. The red colored residue was suspended in hexane, and after sonication for 5 min, the solution was filtered off, the orange powder was collected and dried in vacuum desiccator. Yield: 3.25 g, 99.7%. ^{1}H NMR (600 MHz, [D6] DMSO): δ = 9.20 (s, 2H, 6,6'-bpy), 8.56 (m, 2H, 4,4'-bpy), 8.47 (m, 2H, 3,3'-bpy). ^{13}C NMR (150.78 MHz, [D6] DMSO): δ =169.1 (*C*O-bpy), 155.0 ($C_{5,5'}$), 152.3 ($C_{2,2'}$), 140.2 ($C_{6,6'}$), 135.2 ($C_{4,4'}$), 127.0 ($C_{3,3'}$).

Synthesis of 5,5′-[Glu[G1](OMe)-OMe]$_2$-2,2′-bpy (**2**): 5,5′-bis(chlorocarbonyl)-2,2′-bpy (0.28 g, 1.0 mmol) was dissolved in 10 mL dry CH_2Cl_2. In a separate flask, a dichlormethane (CH_2Cl_2) solution (20 mL) containing H_2N-Glu[G1](OMe)-OMe·HCl, (0.47 g, 2.20 mmol) is mixed with dry triethylamine (Et_3N) (0.33 mL, 2.5 mmol) and stirred for 15 min at r.t.. The former solution was added dropwise to the latter solution. After 12 hours, stirring at r.t., the solution was worked up using saturated $NaHCO_3$ (50 mL), 10% citric acid solution (50 ml), saturated sodium hydrogen carbonate ($NaHCO_3$) (50 ml) and finally with distilled water (50 mL). The organic phase was dried over anhydrous sodium sulfate (Na_2SO_4), filtered and the solvent was evaporated to dryness. Pure compound of **2** was obtained by recrystallization from hexane. Yield: 0.21 g, 38%. TOF MS ESI$^+$ (CH_2Cl_2): *m/z* = 581.3207 $[M+Na]^+$ calc. for $C_{26}H_{30}N_4O_{10}Na$ requires 581.5269. ^{1}H NMR (600 MHz, $CDCl_3$): δ = 9.11 (s, 2H, 6,6′-bpy), 8.53 (s, 1H, 4,4′-bpy), 8.50 (s, 1H, 4,4′-bpy), 8.26 (d, $J_{1,3}$ = 2.31 Hz, 1H, 3,3′-bpy), 8.23 (d, $J_{1,3}$ = 2.31 Hz, 1H, 3,3′-bpy), 7.47 (d, $J_{1,3}$ = 7.25 Hz, 2H, N*H*-Glu), 4.83 (ddd, $J_{1,3}$ = 7.58, 4.95, 2.64 Hz, 2H, αC*H* Glu), 3.81 (s, 6H, αCHCOOCH_3), 3.69 (s, 6H, γCH$_2$COOCH_3), 2.53 (m, 4H, γCH_2 Glu), 2.33 (m, 2H, βCH_2 Glu), 2.22 (m, 2H, βCH_2 Glu). ^{13}C NMR (150.78 MHz, $CDCl_3$): δ = 174.1, 172.3 (CO_{ester}), 165.4 (CO_{amide}), 157.7 ($C_{6,6'}$), 148.3 ($C_{5,5'}$), 136.0, 129.4 ($C_{3,3'}$), 121.3 ($C_{2,2'}$), 53.4 (α*C*H Glu), 52.7, 52.5, 52.0 (COO*C*H$_3$), 30.2 (γ*C*H$_2$ Glu), 26.6 (β*C*H$_2$ Glu).

Synthesis of 5,5′-[Glu[G2](OMe)-OMe]$_2$-2,2′-bpy, (**3**): 5,5′-bis(chlorocarbonyl)-2,2′-bpy (0.28 g, 1.0 mmol) was dissolved in 10 mL dry CH_2Cl_2. In a separate flask, a CH_2Cl_2 solution (20 mL) containing Boc-Glu[G2](OMe)-OMe (1.24 g, 2.20 mmol) was mixed with 1:1 (v/v) trifluroacetic acid (TFA), CH_2Cl_2 solution to remove the Boc protecting group. After 30 min, the resulting solution was neutralized with Et_3N. The solution containing 5,5′-bis(chlorocarbonyl)-2,2′-bpy was added dropwise to H_2N-Glu[G2](OMe)-OMe. After 12 hr, the solution was worked up as described above. Pure compound of **3** was obtained by recrystallization from hexane. Yield: 0.45 g, 40 %.

TOF MS ESI$^+$ (MeOH): *m/z* = 1131.2257 $[M]^+$ calc. for $C_{50}H_{66}N_8O_{22}$ requires 1131.0994. ^{1}H NMR (600 MHz, $CDCl_3$): δ = 9.11 (s, 2H, 6,6′-bpy), 8.54 (d, $J_{1,3}$ = 8.24 Hz, N*H*-Glu), 8.21 (m, 2H, 4,4′-bpy), 8.07 (d, $J_{1,3}$ = 8.57 Hz, 1H, N*H*-Glu), 7.46 (m, 2H, 3,3′-bpy), 7.22 (d, $J_{1,3}$ = 5.61, 2H, N*H*-Glu), 7.12 (m, 2H, N*H*-Glu), 4.70 (m, 4H, αC*H* Glu), 4.56 (m, 1H, αC*H* Glu), 4.34 (m, 1H, αC*H* Glu), 3.79 (s, 12H, αCHCOOCH_3), 3.70 (s, 12H, γCH_2COOCH_3), 2.48 (m, 10H, γCH_2 Glu), 2.31 (m, 9H, γCH_2 and βCH_2 Glu), 2.03 (m, 5H, βCH_2 Glu). ^{13}C NMR (150.78 MHz, $CDCl_3$): δ = 173.9, 173.6, 173.5, 173.2, 173.1, 173.0, 172.7 (CO_{esters}), 170.6 170.4 (*C*O amide), 162.1, 161.6 (*C*O amide proximal to bpy), 157.1, 156.5 ($C_{6,6'}$), 118.7, 117.7 ($C_{5,5'}$), 114.4, 113.5 ($C_{3,3'}$), 110.9 ($C_{2,2'}$), 52.7, 52.6, 52.5, 52.4 (α*C*H Glu), 51.5 (COO*C*H_3), 31.4, 31.3 30.0, 29.9, 29.7, 29.6 (γ*C*H_2 Glu), 28.3, 27.9 26.3, 26.2 (β*C*H_2 Glu).

Synthesis of [(5,5′-[Glu[G1](OMe)-OMe]$_2$-2,2′-bpy)$PtCl_2$] (**4**): Compound **2** (0.1327 g, 0.24 mmol) was suspended in 30 mL ethanol. In a separate flask, K_2PtCl_4 (0.0986 g, 0.24 mmol) is dissolved in 150 mL of water. Then, the latter solution acidity was adjusted to pH = 2.5 with 1M HCl. The two solutions were mixed, and the resultant mixture is refluxed for 4 hrs, the solution color turnd from orange into yellowish-green. After cooling the reaction mixture, the green precipitate was collected by filtration, and washed with cold water (20 mL) and diethylether (100 mL). To remove trace impurities, the complex was crystallized from hot methanol. The solid was dried in vacuum desiccator. Yield: 0.45 g, 55%. M.p. = 244°C (decomp.). TOF MS ESI$^+$ (1:1 (v/v) CH_3OH, H_2O): *m/z* = 824.3464 $[M]^+$ calc. for $C_{26}H_{30}N_4O_{10}PtCl_2$ requires 824.5212. IR (KBr, cm^{-1}): 3450 (br, amide A (non H-bonded)), 3305 (s, amide A (H-bonded)), 1740 (s, CO_{ester}), 1648 (s, amide I), 1545 (s, amide II), 1210 (w, C–O). ^{1}H NMR (600 MHz, [D6] DMSO): δ = 9.89 (s, 2H, 6,6′-bpy), 9.39 (d, $J_{1,3}$ = 7.25 Hz, 2H, N*H*-Glu), 8.82 (m, 4H, 4,4′-bpy and 3,3′-bpy), 4.54 (m, 2H, αC*H* Glu), 3.69 (s, 6H, αCHCOOCH_3), 3.60 (s, 6H, γCH_2COOCH_3), 2.55 (m, 4H, γCH_2 Glu), 2.11 (m, 4H, βCH_2 Glu). ^{13}C NMR (150.78 MHz, [D6] DMSO): δ = 172.9, 171.8 (CO_{ester}), 163.1 (CO_{amide}), 158.4 ($C_{6,6'}$), 148.4 ($C_{2,2'}$), 138.7 ($C_{5,5'}$), 132.5 ($C_{4,4'}$), 124.7 ($C_{3,3'}$), 53.7 (α*C*H Glu), 52.2, 51.4 (COO*C*H_3), 29.8 (γ*C*H_2 Glu), 25.6 (β*C*H_2 Glu). UV-vis (H_2O, λ_{max} (nm): 298 (C=O), 344 (bpy), 438 (MLCT). Anal. Calcd.for $C_{26}H_{30}Cl_2N_4O_{10}Pt$: C 37.87, H 3.67, N 6.80; found C 37.83, H 3.62, N 6.74.

Synthesis of [(5,5′-[Glu[G1](OH)-OH]$_2$-2,2′-bpy)$PtCl_2$] (**5**): Compound **2** (0.2108 g, 0.38 mmol) was suspended in 30 mL ethanol. Solid NaOH (0.6040 g, 1.51 mmol) is dissolved in 1 mL of water, and then is added to the former solution. The mixture was left for 30 min to ensure complete removal of ester group (OMe) from the dendrimer peripherals in **2**. Then, the solution acidity was adjusted to pH = 2.5 using 1M HCl. In a separate flask, the K_2PtCl_4 (0.1566 g, 0.38 mmol) is

dissolved in 150 mL of water. The solution acidity was adjusted to pH = 2.5 with 1M HCl. The two solutions were mixed and the resultant mixture was refluxed for 4 hrs, the solution color changed from light yellow to yellowish-green. After cooling the reaction mixture, the solution pH was adjusted to 5. The readly formed precipitate was collected by filtration, and washed with cold water (20 mL) and diethylether (100 mL). To remove trace impurities, the solid was crystallized from hot ethanol/water mixture. The solid was dried in vacuum desiccator. Yield: 0.08 g, 31%. M.p. = 210°C (decomp.). TOF MS ESI$^-$ (1:1 (v/v) of CH_3OH and H_2O): *m/z* = 767.3202 $[M–H]^-$ calc. for $C_{22}H_{21}N_4O_{10}PtCl_2$ requires 767.4069. IR (KBr, cm^{-1}): 3450 (s, amide A (non H-bonded)), 3290 (s, amide A (H-bonded)), 3055 (w, O–H), 1720 (s, CO_{acid}), 1650 (s, amide I), 1550 (s, amide II), 1220 (s, C–O). ^{1}H NMR (600 MHz, [D6] DMSO): δ = 12.62 (br, 4H, COO*H*), 9.90 (s, 2H, 6,6′-bpy), 9.35 (d, $J_{1,3}$ = 8.20 Hz, N*H*-Glu), 8.85 (m, 2H, 4,4′-bpy), 8.39 (m, 2H, 3,3′-bpy), 4.44 (m, 2H, αC*H* Glu), 2.41 (m, 3H, γCH_2 Glu), 2.13 (m, 3H, γCH_2 and βCH_2 Glu), 2.00 (m, 2H, βCH_2 Glu). ^{13}C NMR (150.78 MHz, [D6] DMSO): δ = 174.6, 174.0 (CO_{acid}), 172.9 (CO_{amide}), 163.0 ($C_{6,6'}$), 147.3 ($C_{2,2'}$), 138.8 ($C_{5,5'}$), 132.6 ($C_{4,4'}$), 124.8 ($C_{3,3'}$), 54.8 (α*C*H Glu), 30.4, 29.0 (γ*C*H$_2$ Glu), 25.8, 24.6 (β*C*H$_2$ Glu). UV-vis (H_2O, λ_{max} (nm): 267 (C=O), 323, 336 (bpy), 390 (MLCT). Anal. Calcd.for $C_{22}H_{22}Cl_2N_4O_{10}Pt$: C 34.39, H 2.89, N 7.29; found C 34.08, H 2.78, N 7.13

Synthesis of [(5,5′-[Glu[G2](OMe)-OMe]$_2$-2,2′-bpy)PtCl$_2$] (**6**): A suspension of **3** (0.0817 g, 0.07 mmol) and *cis*-PtCl$_2$(DMSO)$_2$ (0.0382 g, 0.09 mmol) in 20 mL methanol was sealed in a pressure-resistant vial and reacted at 120 °C for 6 hr. After the vial was cooled down to r.t.. The yellow precipitate was collected by filtration, and then washed with cold acetone (20 mL) and diethylether (100 mL). To remove trace impurities, the complex was crystallized from hot methanol. Finally, the solid residue was freeze-dried affording **6** as yellow powder. Yield: 0.04 g, 38%. M.p. = 204°C (decomp.). TOF MS ESI$^+$ (CH_3OH): *m/z* = 1397.2834 $[M]^+$ calc. for $[C_{50}H_{66}Cl_2N_8O_{22}Pt]^+$ requires 1397.3316. IR (KBr, cm^{-1}): 3455 (br, amide A (non H-bonded)), 3260 (s, amide A (H-bonded)), 1745 (s, CO_{ester}), 1651 (s, amide I), 1552 (s, amide II), 1212 (w, C–O). ^{1}H NMR (600 MHz, [D6] DMSO): δ = 9.99 (s, 2H, 6,6′-bpy), 9.53, 9.80 (m, 2H, N*H*-Glu), 8.82 (m, 2H, 4,4′-bpy), 8.25 (m, 2H, 3,3′-bpy), 4.51 (m, 2H, αC*H* Glu), 3.71 (s, 12H, αCHCOOCH_3), 3.62 (s, 12H, γCH$_2$COOCH_3), 2.39–2.52 (m, 12H, γCH_2 Glu), 2.15–1.82 (m, 12H, βCH_2 Glu). ^{13}C NMR (150.78 MHz, [D6] DMSO): δ =173.5, 173.0, 172.6, 169.9 ($CO_{ester\ and\ amide}$), 161.7, 161.2 ($CO_{amide\ proximal\ to\ bpy}$), 156.5, 156.0 ($C_{6,6'}$), 118.3, 117.2 ($C_{5,5'}$), 113.9 ($C_{3,3'}$), 112.9 ($C_{2,2'}$), 52.1 (α*C*H Glu), 51.0, 45.0 (COO*C*H$_3$), 30.9, 29.5 (γ*C*H$_2$ Glu), 27.5, 25.8 (β*C*H$_2$ Glu). UV-vis (H_2O, λ_{max} (nm): 298 (C=O), 344 (bpy). Anal. Calcd.for $C_{50}H_{66}Cl_2N_8O_{22}Pt$: C 42.98, H 4.76, N 8.02; found C 42.73, H 4.93, N 7.90.

Synthesis of [(5,5′-[Glu[G2](OH)-OH]$_2$-2,2′-bpy)PtCl$_2$] (**7**): A suspension of **3** (0.1131 g, 0.10 mmol) in 1 mL methanol was allowed to react with an aqueous solution (1 mL) of NaOH (0.0320 g, 0.80 mmol) for 30 min at r.t. The solution pH was adjusted to 2.5 with 1 M HCl. The resulting solution was transferred to a pressure-resistant vial containing *cis*-PtCl$_2$(DMSO)$_2$ (0.0.0530 g, 0.13 mmol) in methanol (20 mL). The solution was heated up to 120 °C for 6 hr. After the vial was cooled down to r.t., the solution pH was adjusted to 3. The yellow precipitate was collected by filtration, and then washed with cold acetone (20 mL) and diethylether (100 mL). Purification of **7** was carried out by crystallization from hot ethanol/water mixture. The resulting residue was freeze-dried affording **7** as yellow powder. Yield: 0.03 g, 27%. M.p. = 147°C (decomp.). TOF MS ESI$^-$ (CH_3OH/H_2O): *m/z* = 653.3040 $[M–3H+Na]^{2-}$ calc. for $[C_{42}H_{47}Cl_2N_8NaO_{22}Pt]^{2-}$ requires 653.4189. IR (KBr, cm^{-1}): 3480 (s, amide A (non H-bonded)), 3260 (s, amide A (H-bonded)), 3065 (w, O–H), 1725 (s, CO_{acid}), 1650 (s, amide I), 1545 (s, amide II), 1214 (s, C–O). ^{1}H NMR (600 MHz, [D6] DMSO): 9.87 (s, 2H, 6,6′-bpy), 9.80, 9.49 (d, $J_{1,3}$ = 7.45 Hz, 2H, N*H*-Glu), 8.90, 8.79 (m, 2H, 4,4′-bpy), 8.41, 8.30 (m, 2H, 3,3′-bpy), 8.14 (m, 4H, N*H*-Glu), 4.50–4.18 (br m, 6H, αC*H* Glu), 3.30, 2.25 (m, 12H, γCH_2 Glu), 2.08–1.92 (m, 12H, βCH_2 Glu). ^{13}C NMR (150.78 MHz, [D6] DMSO): 174.2, 174.0, 169.7, 169.2 ($CO_{ester\ and\ amide}$), 161.4, 161.0 ($CO_{amide\ proximal\ to\ bpy}$), 155.8 ($C_{6,6'}$), 145.8 ($C_{2,2'}$), 119.2 ($C_{5,5'}$), 117.3 ($C_{4,4'}$), 113.0 ($C_{3,3'}$), 54.0 (α*C*H Glu), 31.1, 30.2 (γ*C*H$_2$ Glu), 27.7, 26.0 (β*C*H$_2$ Glu). UV-vis (H_2O, λ_{max} (nm): 265 (C=O), 320, 334 (bpy), 390 (MLCT). Anal. Calcd.for $C_{42}H_{50}Cl_2N_8O_{22}Pt$: C 39.26, H 3.92, N 8.72; found C 38.98, H 3.96, N 8.67.

Results and discussion

Design principles: The platinated peptide dendrimer conjugates designed in this report, shown in Fig. 1a, were of generation 1 (G1(OH), **5**) and generation 2 (G2(OH), **7**). In addition, the parent complex (G0(OH), **1**) was prepared as a control to ensure the effect of tethering the peptide residues. The photo-system used to induce water reduction to molecular hydrogen by catalyst **1**, **5** and **7** is shown in Figure. 1b.

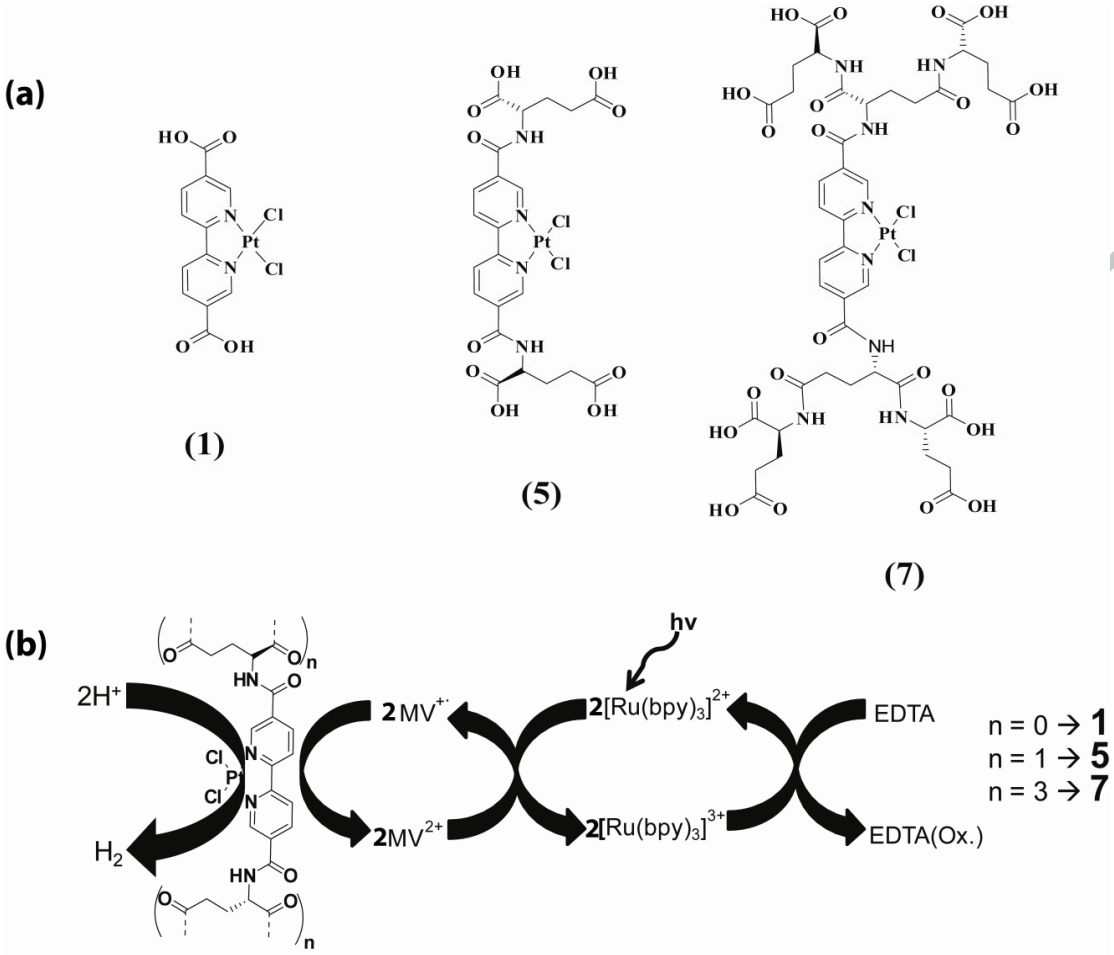

Figure 1. (a) Molecular Pt(II) complexes: The $PtCl_2$(5,5'-(COOH)-2,2'-bpy) (**1**, G0(OH)), the glutamic acid dendron in **5** (G1(OH)) is of generation 1 and in **7** (G2(OH)) is of generation 2. (b) Schematic representation of the optical and chemical processes for visible-light driven H_2 evolution in a multicomponent system. The components are a sacrificial electron donor (EDTA), metal complex sensitizer $[Ru(bpy)_3]^{2+}$ (bpy: 2,2'-bipyridine), an electron mediator (methylviologen, MV^{2+}: *N*,*N*'-dimethyl-4,4-bipyridinium) in acetic acid/sodium acetate buffer (pH = 5) and a hydrogen generating catalyst (**1**, **5** and **7**).

The inner coordination sphere of the designed complexes utilizes $PtCl_2$(bpy) moiety as probe catalyst. The outermost coordination sphere (peripheral) was decorated with carboxyl groups. In the catalytic buffer solution (pH = 5), Figure 1b, the carboxyl groups were fully dissociated (pK_{aGlu}(COOH) = 3.5, 4.1).[21] The carboxylate groups facilitate catalyst solubility in water and enhance proton-electron transfer (PET) by increasing the local concentration of protons and $MV^{+\bullet}$ at the peripheral.[27] The increasing number of carboxylates (**7>5>1**) was utilized to test the effect of carboxylate group in catalytic performance, presumably by increasing the number of associated $MV^{+\bullet}$ species.[18] The role of peripheral group type in catalyst activity was further elaborated by designing platinated peptide dendrimer conjugates having methoxy groups at the outermost coordination sphere, namely (G1(OMe), **4**) and generation 2 (G2(OMe), **6**), Scheme 1.

The middle coordination sphere in the peptide conjugates consisted of amide groups, which act as proton relay between the innermost and outermost coordination spheres.[14, 28] The methylene

alkyl groups of the *L*-glutmaic acid side chain modulated the dielectric around the Pt-center by creating a hydrophobic core,[21] which with increasing dendrimer generation number (layers) the methylene group number increases. The peptide layers of G1 and G2 are known to adopt open conformation in water. Therefore, facilitate shuttling of electons, protons (H^+) and releasing out $H_{2(g)}$. To this end, we will address the following structural variations of peptide dendrimers on the H_2-evolving activity of the $PtCl_2$(bpy) core: (i) Effect of amide functionality on the inner coordination sphere (G0(OH) *vs*. G1(OH), G2(OH)). (ii) Number and type of peripheral groups of the outermost coordination sphere, Gn(OMe) *vs*. Gn(OH) for n = 1, 2, and (iii) increasing peptide layers around the core (encapsulation).

Synthesis: In the detailed syntheses, the peptide conjugates were prepared by applying a complexation reaction between Pt-precursor with glutamic acid dendrimers having bpy at the core. The 5,5'-dicarboxyl-2,2'-bipyridine (dcbpy) ligand is synthesized by oxidation of 5,5'-dimethyl-2,2'-bipyridine using the reported literature procedure, which is depicted in scheme 1.[24] The platination of dcbpy ligand using *cis*-$PtCl_2(DMSO)_2$ precursor, afforded $Pt(dcbpy)Cl_2$ (G0(OH), **1**) complex as orange solid in good yield (44%), Scheme 1.

The synthesis of the G2 dendrons was demonstrated by the convergent growth approach using conventional solution phase peptide coupling chemistry of N-α-Boc-*L*-Glu(OH)-OH and H_2N-*L*-Glu(OMe)-OMe of 1:2 stoichiometry in dry CH_2Cl_2, Scheme S1. In the following step, the G1 and G2 dendrons were coupled with 5,5′-bis(chlorocarbonyl)-2,2'-bipyridine, in presence of Et_3N in dry CH_2Cl_2. The coupling reaction G1 (**2**) and G2 (**3**) dendrimers, as white solid products in (38%) and (40%) yields, respectively, Scheme 1.

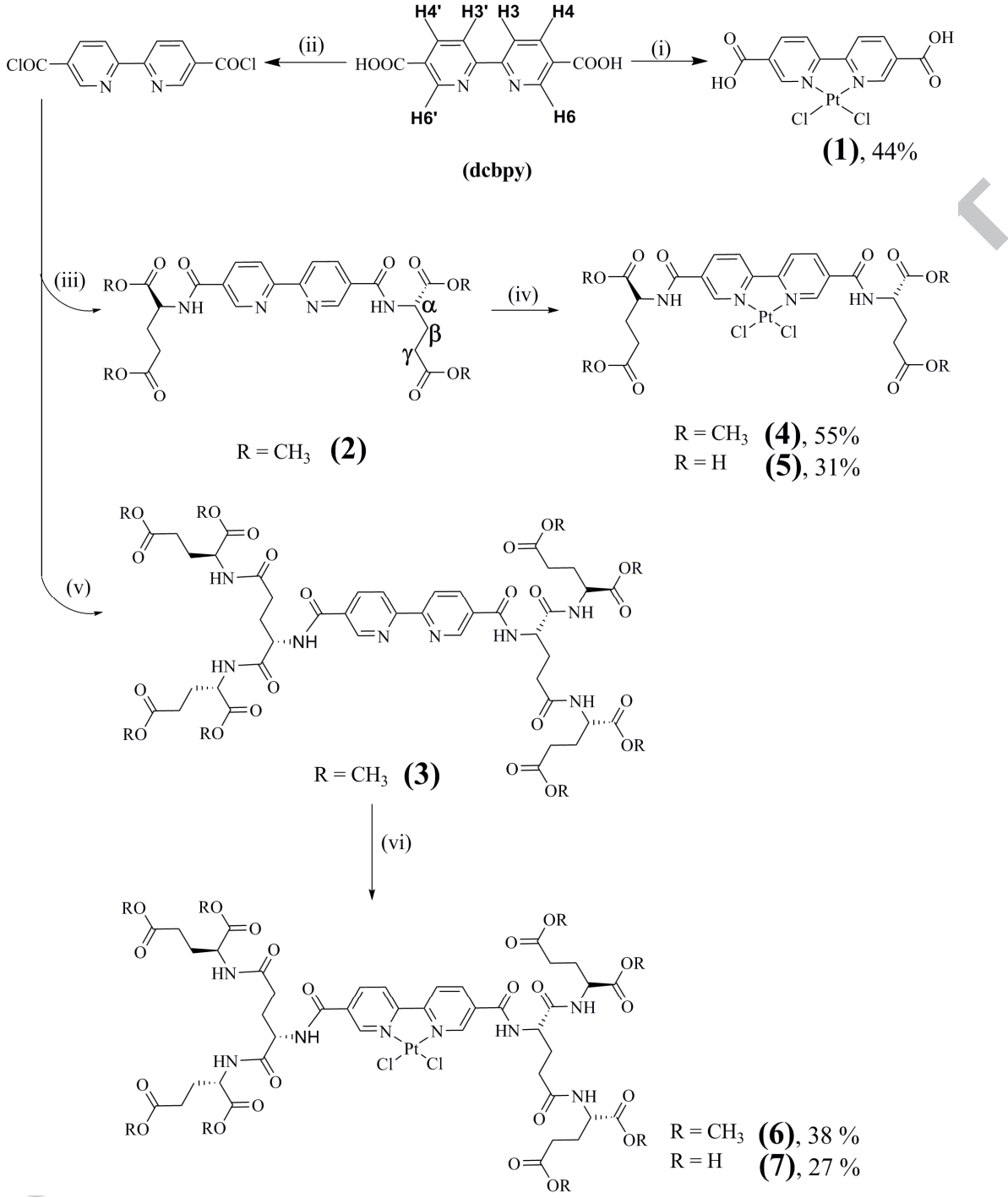

Scheme 1. Synthesis of compounds **1**–**7**. (i) *cis*-$PtCl_2(DMSO)_2$, MeOH, 120 °C. (ii) $SOCl_2$, THF, 40°C (iii) H_2N-Glu(OMe)-OMe·HCl/Et_3N. (iv) Conjugate **4**: K_2PtCl_4, EtOH/H_2O (pH = 2.5), reflux. Conjugate **5**: (1) NaOH in wet methanol, 15 min, adjustment to pH = 2.5. (2) K_2PtCl_4, EtOH/H_2O, (pH = 2.5), reflux. (v) Compound **3**, Boc group removal: TFA, neutralization of excess TFA by Et_3N. (iv) Conjugate **6**: *cis*-$PtCl_2(DMSO)_2$, MeOH, 120 °C. Conjugate **7**: (1) NaOH in wet methanol, 15 min, adjustment to pH = 2.5. (2) *cis*-$PtCl_2(DMSO)_2$, MeOH, 120 °C.

The synthesis of Pt-conjugate G1(OMe) (**4**) was conveniently achieved by reacting K_2PtCl_4 with compound 2 under refluxing in ethanol/H_2O mixture. Purification of **4** was readily achieved by retro crystallization, affording **4** as green solid in good yield (55%). The Pt-conjugate G1(OH) **5** was prepared by removing methyoxy group in **2** using base hydrolysis,

followed by a reaction of the resulting ligand to K_2PtCl_4 under refluxing in ethanol/H_2O mixture to afford conjugate **5** as green solid in acceptable yield.

When the synthetic strategy described above was employed to prepare Pt-conjugates G2(OMe) (**6**) and G2(OH) (**7**), a black solid, attributable to colloidal platinum, was obtained.[29] Therefore, Pt-conjugates **6** and **7** were prepared by complexation of **3** to *cis*-$PtCl_2(DMSO)_2$ in methanol in an autoclave at 120°C. The final products were obtained as orange solids in acceptable yields, (38%) and (27%), respectively.

The resulted products have shown different solublity behaviors. For example, complex **1** was soluble in DMSO, slightly insoluble in water and completely insoluble in either methanol or CH_2Cl_2. However, conjugates **4** and **6** were soluble in either methanol or CH_2Cl_2 but insoluble in water. Conjugates **5** and **7** were soluble in water and methanol but insoluble in chlorinated solvents.

Characterization: The successful formation of the complexes **1**, **4**–**7** were confirmed by mass spectrometry, elemental analysis, UV-vis, infrared (IR), and ^{1}H-, ^{13}C-NMR spectroscopies. The full ^{1}H-, ^{13}C-NMR assignments were made on the basis of 2D TOCSY and HSQC. The relevant spectroscopic data are summarized in Table 1.

Table 1. Selected spectroscopic characterization of Pt complexes **1** and **4**–**7.**

	UV-vis (λ, nm)[a]	^{1}H NMR (ppm)[b]				IR (cm^{-1})[c]			
Complex	Pt→bpy	H6, H6'	N*H*$_{bpy}$[d]	COO*H*	COOC*H*$_3$	NH	CO_{acid}	CO_{ester}	CO_{amid}
1	370	9.99	-	-		-	1700	-	-
4	435	9.89	9.39	-	3.69, 3.60	3450, 3305	-	1740	1648
5	390	9.90	9.35	12.62	-	3450, 3290	1720	-	1650
6	438	9.99	9.53, 9.80	-	3.70, 3.62	3455, 3300	-	1745	1651
7	390	9.87	9.80,9.49	-	-	3480, 3260	1725	-	1650

[a]Recorded in water. [b] 5 mM concentration in [D6] DMSO for complexes **1**, **5** and **7**. For complexes **4** and **6**: 5 mM in $CDCl_3$ at 24 °C. [c] IR recorded in KBr. [d] amide proximal to pyridine ring.

The observed mass spectrometry data well supported the validity of the formulations proposed for **1** and **4**–**7** Figs. S1–S3. The isotopic distribution patterns of the platinated products clearly revealed the coordination of the platinum(II) to the bpy unit, Figures S1,S2. The elemental analyses results further confirm the composition as well as purity of the synthesized complexes.

The UV-vis spectra for **1** and **4**–**7** displayed the characteristics absorption of the existed chromophoric groups. The carbonyls n→π^* transition of amides, acids and esters were at 255–290 nm range, the doublet peak of bpy ($\pi\rightarrow\pi^*$ transition) was at 315–344 nm and the broad low intense of Pt→bpy MLCT was at 360–400 nm, Fig. S4. These values were in good agreement to the reported absorptions of related *cis*-$PtCl_2$(bpy) complexes.[16, 30] The variation on the perceived

color of solid **4** and **5** (green) and of solid **1**, **6** and **7** (orange), Figure S5, which has been preserved in solution, is attributed to a possible aggregations of the monomers in **4** and **5** "polymeric stacking". In contrast, the orange colored most likely indicates a "monomeric" form in complexes **1**, **6** and **7**.[31, 32]

Infrared spectroscopy (IR) has clearly shown the presence of the carboxyl and ester functional groups in the Pt-complexes. The carboxyl group appeared in the region (1700-1720 cm^{-1}) for the complexes **1**, **5**, and **7**. The ester group appeared at 1740 cm^{-1} for the complexes **4** and **6**, Table 1 and Figs. S4–S6. Additionaly, the broad peak in the region 3600–2600 cm^{-1} were assigned to the OH stretching modes of the carboxyl groups.[33] Complex **1** and Pt conjugates **4**–**7** exhibit a typical amide A band at 3400 cm^{-1} and amide I at 1650 cm^{-1} as shown in Table 1.

The ^{1}H NMR of **1** exhibits a downfield chemical shift of bpy proton peaks compared to the free dcbpy ligand, Figure 2. Upon complexation, the singlet peak of H6,H6' (6,6'-bpy) protons, Scheme 1, was downfield shifted (δ9.29→δ9.99), Figure 2. This shift is related to the formation of coordinate bond to the electron withdrawing Pt^{2+} center. The chemical shift of the H6, H6' singlet peak has subsequently monitored the progress of the platination reaction in complexes **4**–**7**.

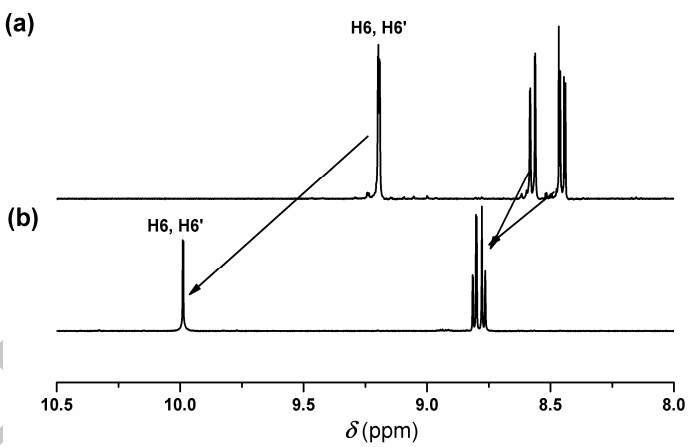

Figure 2. Partial ^{1}H NMR spectra of (a) dcbpy ligand, (b) (dcbpy)$PtCl_2$ (**1**). (5 mM in [D6] DMSO).

The ^{1}H NMR of **2** have proven the presence of the characteristic proton signals of the bpy ring and the glutamic amino acid fragments, Figs. 3a and S8. The ^{1}H NMR of **4**, Fig. 3b, confirms successful platination of **2** as evidenced by the downfield shift of H6,H6' singlet peak. The ^{1}H NMR spectrum of conjugate **5**, Figure. 3c, have shown lack of the siganls of the methyoxy ester groups at δ3.69 and δ3.60. In addition, a broad resonance peak appears at δ12.62, Fig. S7, and is assigned to the carboxyl OH groups in **5**.

The ^{1}H NMR of conjugate **6** and **7** exhibits similar changes in chemical shift at the H6,H6' singlet peak, Fig. S9. The ^{13}C-NMR spectra of complexes **1** and **4**–**7** exhibit the peak for the carbonyl

carbon derived from the carboxyl group at ~ δ176–δ173, Fig. S10, while for the carbonyl carbon of the ester group appears at ~ δ171, Fig. S11.

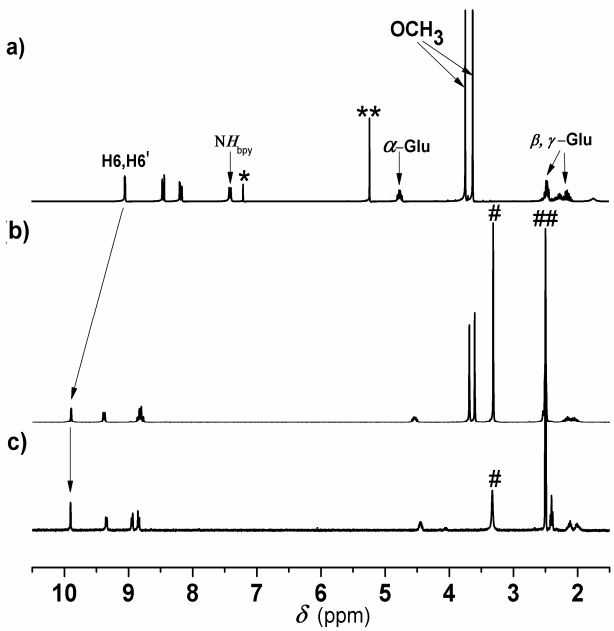

Figure 3. ^{1}H NMR spectra of (a) compound **2** (5 mM in $CDCl_3$). (b) Conjugate **4** (5 mM in [D6] DMSO) and (c) conjugate **5** (5 mM in [D6] DMSO). * Residual $CDCl_3$, ** residual CH_2Cl_2 in $CDCl_3$, $^{\#}$ residual [D6] DMSO, $^{\#\#}$ residual water in [D6] DMSO.

DFT Calculations: Density functional theory (DFT) and Time-dependent density functional theory (TD-DFT) calculations were carried out on the ground state of **1** and **5** in their monomeric form. The calculation has utilized polarizable contium model (PCM) to account for solvent effects in aqueous media. Optimized structure of **7** was not attainable, due to difficulties in obtaining molecular structure that yielded satisfactorly converged ground state. The calculated UV-Vis spectrum for **1** have shown intense band at 310 nm and moderatly intense band at 428 nm as a result of several electronic transitions between molecular orbitals and virtuals (Figure 5a and Table S1). On the other hand, complex **5** have shown three intense absorption bands at 384, 332 and 292 nm (Figure 5b and Table S3). Inspite of the lack of agreement between the experimental and the calcluated UV-Vis spectra (Fig. S4), the calculated spectra reproduce the main features of the experimental spectra.

The long wavelength transition in **1**, at 370 nm (experimentally) which was reproduced at 428 nm theoretically, is due to transition from H-1 to LUMO (Table S2). The molecular orbital analysis listed in Table S2, indicates that H-1 is 52% on the Pt core and 36% on Cl, whereas, the LUMO is mainly located on the bpy lignad (96%). Thus, the long wavelength transition is a contribution of metal to ligand charge transfer (MLCT) and halide (Cl) to ligand charge transfer (XLCT).[31] The

calculation shows that the strongest absorption line in this absorption band is mainly due the transition from H-5 to LUMO, in which 99% of H-5 and 96% of LUMO are located at the bpy ligand. The result indicates a ligand centered charge transitions (LC). Similar molecular orbital analysis for **5** confirms that the long wavelength is MLCT and XLCT while shorter wavelength bands are due to LC transitions.

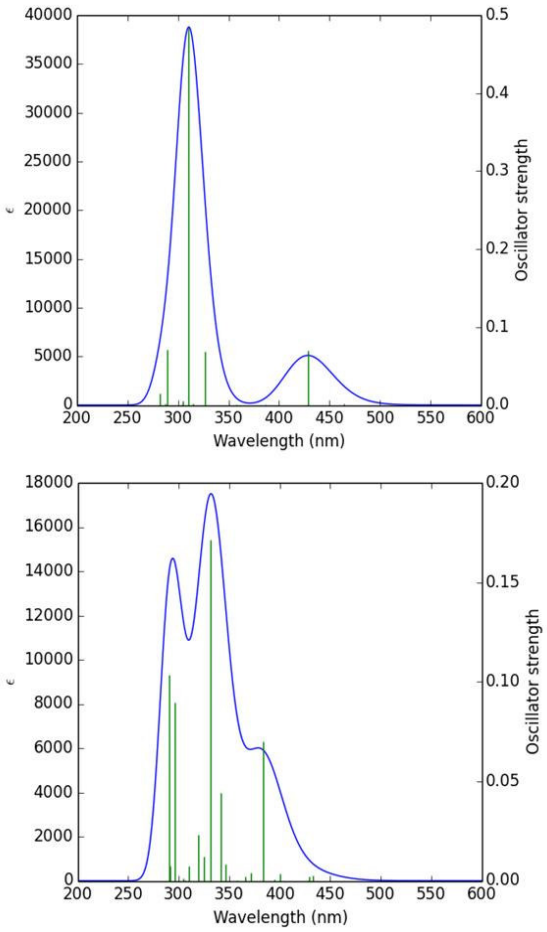

Figure5: Calculated UV-is spectra for the ground state of (a) **1** (top), and (b) **5** (bottom).

The DFT study suggests that building amide functional groups in the bpy ligand alters its electronic properties, this effect is clearly noticed from the shift in MLCT band from 428 nm in **1** to 384 nm in **5** and further confirmed from the calculated $\Delta E_{(\text{LUMO-HOMO})}$ = 3.32eV and 3.65eV for **1** and **5** respectively. It is expected that a similar change in the electronic properties would be occured to bpy in **7** due to the similarity of the properties of the attached amide groups, this assumption is supported by the identcal abosrption behavior of complex **5** and **7** in their UV-Vis spectra shown in Fig. S4.

In conclusion, first, the experimental and quantum theortical calculations both indicates their is a change in HOMO-LUMO gap upon amide bond formation for **5** and **7** and regardless of the complex aggregation form. Secondly, The bathochrmic shift in MLCT transition, obtained from the UV-Vis spectra shown in Fig. S4, for **5** and **7** compared to **1** suggests lowering of the energy gap. Finally, the increasing dendrimer generation number (peptide branches) impacts the electronic properties of the first coordination sphere, this is further evidenced from the emission spectra of the complexes **1**, **5** and **7**, Fig. S16. Although the luminescence spectra displayed similar emission features, there intensity are in the order **5** > **1** > **7**.[34]

Conformational analysis: The asymmetric nature and conformational flexibility in glutamic amino acid side chains should provide different magnetic environments for the H6,H6′ and NH_{bpy} protons. Interestingly, the ^{1}H-NMR spectra for **4** and **5** revealed a sharp, similar chemical shifts for the H6,H6′ and NH_{bpy} protons as well as for the α-, β-, and γ-Glu protons, Figures 3b and 3c and Table 1. This observation indicates a C_2 symmetry in **4** and **5**, therefore, it is likely that the glutamic acid side chains have identical orientation on both sides of bpy, Scheme 1.

For **6** and **7** conjugates, the ^{1}H-NMR spectra have confirmed the presence of multiple peaks for the H6,H6′ and NH_{bpy} protons, (Figure S10 and Table 1), in addition, the Glu protons on G2 dendrons exhibited broad chemical shifts, suggesting an asymmetric arrangement of G2 dendrons. This is likely due to existence of several, non-identical orientations of the glutamic acid side chains in G2 dendrons, Scheme 1.

To provide insight into a potential aggregation in conjugates **4** and **5**,[32, 34] variable temperature (VT) UV-Vis study have been carried out. In case of aggregation, several possible intermolecular interactions of the $PtCl_2$(bpy) core were suggested, like π-π (aromatic of bpy) interactions or $d_{z^2} - d_{z^2}$ (Pt-Pt) interactions.[35] One would expect that with increasing temperature, the thermal energy would drive weakening the intra-complex interactions present in **4** and **5**. Subseqently this affects the electronic properies of the stacked complexes, resulting in changes on their UV-vis spectra, scheme 2.

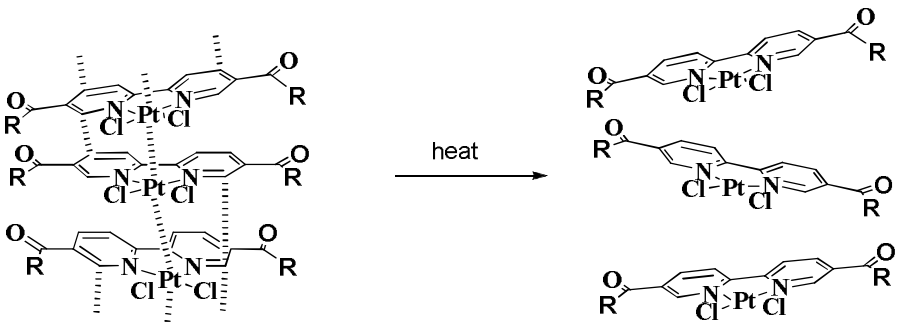

Scheme 2: Depiction of possible stacking modes on conjugate **5** and their conversion to monomeric species upon heating. The possible stacking interactions are: π-π (aromatic bpy), $d_{z^2} - d_{z^2}$ (Pt-Pt), R = H2N-Glu(OH)-OH.

The impact of varying the temperature on the absorbance spectrum of **5** was studied and the results were compared to the results obtained from **1** and **7**. Analyses of the UV-vis spectra of **5** at 25, 40, 60 and 80°C revealed that the ligand based (LC) transition, which appears as doublet absorption peaks (323 nm, 336 nm), exhibited a bathochromic shift (330 nm, 343 nm) upon raising the temperature from 25°C to 40°C, Figure 6. Futhermore, upon increasing the temperatue to 60 and 80°C, the LC band has blue shifted to 320 nm 334 nm. It has been described that in systems containing aromatic chromophores, the π→π* transitions exhibit a hypochromism and bathochromic shifts in case of strong π*-orbital coupling interactions, while the hypsochromic shift is an indicative of weak π*-orbital coupling interactions.[36] It seems that complex **5** starts to deaggregate from "polymeric" stacking → "monomeric" at 60 °C, evidenced by the blue shift in π→π* transition peaks, this phase transition event of $PtCl_2$(bpy) is associated with an increasing in solution scattering. The LC band in **1** and **7** display a small blue shift at all temperature values, which indicates the absence of stacking, Figures S12,S13.

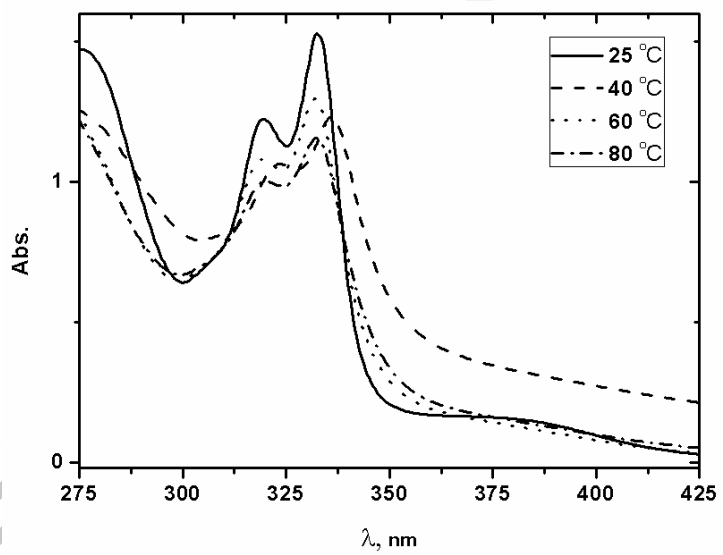

Figure 6: Varible temperature (VT)-UV-vis of **5** (1mM)

In conclusion, the ^{1}H-NMR and VT-UV-Vis studies confirm the stacking modes of monomers in **4** and **5** which presumably gives rise to the green color of the complexes in the solid state and solution.[42] Unfortuntly, we have been unable to run VT-^{135}Pt NMR to further confirm Pt-Pt interactions in the aggregated mode of **4** and **5,** therefore we will speculate its existance based on literaure investigation on $PtCl_2$(bpy) system and other related systems.[30, 35, 37]

Catalytic study: The catalytic activities of dendrimer **1** and **4**–**7** were evaluated employing these complexes in the photochemical H_2 evolution from water. This study was performed according to

our previously reported conditions.[24] However, applying the same catalytic process using complexes **4** and **6** were unsuccessful due to their poor solubility in aqueous media. In general, for the complexes **1**, **5** and **7**, an aqueous acetate buffer solution of each complex (1.0 M, pH = 5), methylviologen, $[Ru(bpy)_3]^{2+}$, and sodium chloride, were used to study their catalytic activities, (Figure1b). The induction period (~5–10 min) observed in each experiment is considered to populate one-electron-reduced form of methylviologen (i.e., $MV^{+\cdot}$), (Figure S11). Furthermore, this step ensures the absence of hydrogen evolution activity due to Pt nanoparticles.[24]

Table 2. Summary of the catalyst activity parameters.

Complex No.	Initial rate (mL/min)	Turnover ferquency ($\times 10^{15}$ H_2 molecule/sec)
1	0.004	7
5	0.004	14.7
7	0.004	3.8

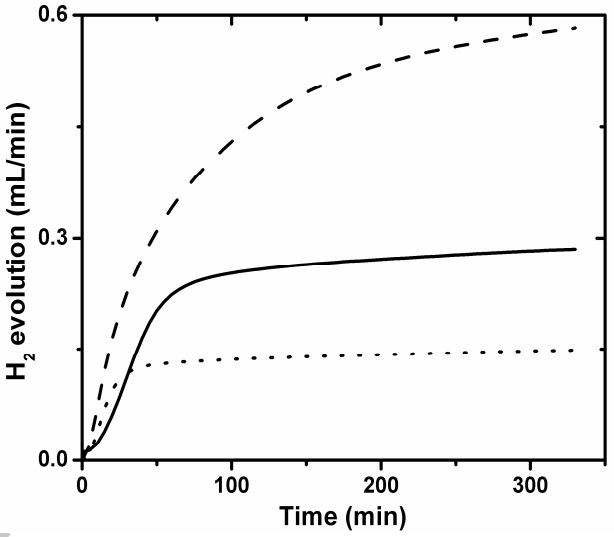

Figure 7. Photochemical H_2 production of **1** (solid), **5** (dashed), **7** (dotted).

The number of turnovers frequencies (TOFs) of catalysts **1**, **5** and **7** are estimated on the basis of the total amount of H_2 evolved after 5 hr and the amount of each catalyst (1 µmol), (Figure 7 and Table 2). The catalytic activity for H_2 formation is found to decrease in the order of **5** > **1** > **7**.

The catalytic behaviour in $PtCl_2$(bpy) systems is likely to be accelerated by formation of dinuclear complex intermediate, presumbly using $d_{z^2}(Pt) - d_{z^2}(Pt)$ interactions. It has been shown that the overall catalytic activity of Pt-molecular catalyst for H_2-evolution from water is accelerated by adding extra Pt-based complexes as co-catalyst,[38] implying the formation of heteroleptic intermediate utilizing Pt···Pt bond. The observation was explained by The properties of **5**, including distinct green color, rigid conformation of the glutamic residues and its dissociation in responce to heating, supports the hypothesis of aggregate formation. The higher H_2 activity in **5** in

comparison to **1** and **7** further indicates the existance of Pt-Pt interactions though it is not proven in this study. This interaction seems to be in favor for the case of G1 dendrons, while the G2 dendron branches prevent the formation of aggregates in **7**, most likely due to steric hindrance.

The number of carboxylate groups at the dendrimer peripherals in **7** has no effect on inceseaing the H_2 evolution activity. In the contrary, the G2 dendron branches seems to isolate the $PtCl_2$(bpy) core from the surrounding aqueous medium (encapsulation effect). Similar encapsulation effects have been reported in Ferrocene-glutamic acid dendrimers.[21]

Conclusions

Four new Pt-glutamic acid dendrimer conjugates have been synthesized **4**-**7**. The natural *L*-glutamic amino acid layers were built into the bpy ligand framework (G0(OH), **1**). The G0(OH) is the unmodified parent complex $PtCl_2$(5,5'-dicarboxylic acid-2,2'-bipyridine). The *N*-terminus of the dendrimer is attached to the G0(OH) utilizing amide bond formation at the 5,5'-position, whereas the *C*-terminus are terminated with methoxy (OMe) or carboxy (OH) groups. These dendrimers are of generation 1, (G1(OMe), **4** and G1(OH), **5**, and generation 2 (G2(OMe), **6** and G2(OH), **7**. The structure and composition of these conjugates have been determined by various spectroscopic techniques.

The amide bond formation has altered the electronic properties of the bpy ligand indicated by the DFT calculations. The type of functional group (ester *vs*. acid) at the dendrimers peripheral influences the solubility behavior of the synthesized conjugates in water. The conformational study has indicated a aggregation order of generation 1 conjugates (**4**,**5**) evidenced by their apparent color, rigidity and the alteration in their electronic properties in response to temperature.

The H_2-evolution photocatalytic activitiy of water soluble conjugates **1**, **5** and **7** are well correlated to the ability of the conjugate to form a polynuclear structure. Apparently, the increasing number of carboxylic acid groups at the peripheral has no influence on increasing H_2-activities, instead the barrier for electron and proton transfer has increased with bulky G2 dendrimers (encapsulation effect). The work presented in this article leaves the question of possible existence of Pt-Pt interactions unanswered in Pt(II)-*L*-glutamic acid conjugates. Currently, we are developing systems of Pt(II)-*L*-aspartic acid conjugates. Arguably, these conjugates will have less steric hindrance and would allow facile aggregate formation.

Acknowledgments

A. Lataifeh wishes to thank University of Western Ontario/Chemistry Department for ASPIRE award and Dr. T. Ashboul/ Friedrich Schiller-University of Jena for runing the elemental analysis. A. Lataifeh is grateful to financial support from Tafila Technical University(TTU)/Jordan (grant number: 150/2012). This work was funded by Natural Sciences and Engineering Research Council

of Canada (NSERC) and the University of Western Ontario (UWO). This work was partly supported by the International Institute for Carbon Neutral Energy Research (WPI-I2CNER), sponsored by the World Premier International Research Center Initiative (WPI), MEXT, Japan.

References

[1] A.K.-W. Chan, M. Ng, Y.-C. Wong, M.-Y. Chan, W.-T. Wong, V.W.-W. Yam, Journal of the American Chemical Society, 139 (2017) 10750-10761.
[2] M.E.M.D. Stefan Harmsen, Zoltan Nemes, Marie Lacombe, Balint Szokol, Janos Pato, Gyoorgy Keri, Laszlo Orfi, Gert Storm, Wim E. Hennink, Robbert J. Kok, Bioconjugate Chemistry, 22 (2011) 540-545.
[3] Y.L. Zhen Feng, Haifeng Ye, Jing Huang, Xu Guang Xi, Zirong Wu, Cancer Science, 101 (2010) 2476-2482.
[4] J.-J. Zhong, C. Yang, X.-Y. Chang, C. Zou, W. Lu, C.-M. Che, Chemical Communications, 53 (2017) 8948-8951.
[5] M.Y. Hayato Ogawa, Dalton Transaction, 42 (2013) 625-629.
[6] S.M.V. Sergey Abramkin, Michael A. Jakupec, Markus Galanski, Nils Metzler-Nolte, Bernhard K. Keppler, Dalton Transaction, 41 (2012) 3001-3005.
[7] Z. Kokan, B. Perić, G. Kovačević, A. Brozovic, N. Metzler-Nolte, S. Kirin, European Journal of Inorganic Chemistry, (2017).
[8] H.-B.K. Patrycja W. Galka, Journal of Organometallic Chemistry, 674 (2003) 24-31.
[9] A.D. Bojana Ginovska-Pangovska, Matthew L. Reback, John C. Linehan, Wendy J. Shaw, Accounts of Chemical Reserach, 47 (2014) 2621-2630.
[10] T.H. Akira Onoda, Current Opinion in Chemical Biology, 25 (2015) 133-140.
[11] S. Fukuzumi, Y.-M. Lee, W. Nam, Coordination Chemistry Reviews, (2017).
[12] M.P.S. Monte L. Helm, R. Morris Bullock, M. Rakowski DuBois, Daniel L. DuBois, Science, 333 (2011) 863-866.
[13] B.G.-P. Matthew L. Reback, Ming-Husn Ho, Avijita Jian, Thomas C. Squier, Simone Raugei, John A. S. Roberts, Wendy J. Shaw, Chemistry Europian Journal, 19 (2013) 1928-1941.
[14] J.A.S.R. Arnab Dutta, Wendy J. Shaw, Angewandte Chemie International Edition, 53 (2014) 1-6.
[15] B.S. Michael G. Pfeffer, Grigory Smolentsev, Jens Uhlig, Elena Nazarenko, Julien Guthmuller, Christian Kuhnt, Maria Wachtler, Benjamin Dietzek, Villy Sundstrom, Sven Rau, Angewandte Chemie International Edition, 54 (2015) 1-5.
[16] S.M. Kosei Yamauchi, Ken Sakai, Dalton Transaction, 40 (2011) 12447-12449.
[17] V.A. Carole Baffert, Marc Fontecave, Inorganic Chemistry, 46 (2007) 1817-1824.
[18] G.A. Makoto Ogawa, Shigeyuki Masaoka, Heinz-Bernhard Kraatz, Ken Sakai, Chemistry Europian Journal, 17 (2011) 1148-1162.
[19] J.S.I. Petr Niederhafner, Jan Ježek, Journal of peptide science, 11 (2005) 757-788.
[20] L.-W.L. Sergei A. Vinogradov, David F. Wilson, Chemical Europian Journal 5(1999) 1338-1347.
[21] Y.-T.L. Francis E. Appoch, Heinz-Bernhard Kraatz, Langmuir, 22 (2006) 10515-10522.
[22] W.H. von M. Brenner, Helvetica Chimica Acta, 136–137 (`1953) 1109–1114.
[23] D.S. Tarbell, Yamamoto, Yutaka, Pope, Barry M, Proceedings of the National Academy of Sciences, 69 (1972) 730-732.
[24] H. Ozawa, Haga, Masa-aki, Sakai, Ken, Journal of the American Chemical Society, 128 (2006) 4926-4927.
[25] N.M.T. O'boyle, Adam L Langner, Karol M, Journal of computational chemistry, 29 (2008) 839-845.

[26] G.W.T. M. J. Frisch, H. B. Schlegel, G. E. Scuseria, M. A. Robb, J. R. Cheeseman, G. Scalmani, V. Barone, B. Mennucci, G. A. Petersson, H. Nakatsuji, M. Caricato, X. Li, H. P. Hratchian, A. F. Izmaylov, J. Bloino, G. Zheng, J. L. Sonnenberg, M. Hada, M. Ehara, K. Toyota, R. Fukuda, J. Hasegawa, M. Ishida, T. Nakajima, Y. Honda, O. Kitao, H. Nakai, T. Vreven, J. A. Montgomery, Jr., J. E. Peralta, F. Ogliaro, M. Bearpark, J. J. Heyd, E. Brothers, K. N. Kudin, V. N. Staroverov, T. Keith, R. Kobayashi, J. Normand, K. Raghavachari, A. Rendell, J. C. Burant, S. S. Iyengar, J. Tomasi, M. Cossi, N. Rega, J. M. Millam, M. Klene, J. E. Knox, J. B. Cross, V. Bakken, C. Adamo, J. Jaramillo, R. Gomperts, R. E. Stratmann, O. Yazyev, A. J. Austin, R. Cammi, C. Pomelli, J. W. Ochterski, R. L. Martin, K. Morokuma, V. G. Zakrzewski, G. A. Voth, P. Salvador, J. J. Dannenberg, S. Dapprich, A. D. Daniels, O. Farkas, J. B. Foresman, J. V. Ortiz, J. Cioslowski, D. J. Fox, in, 2010.
[27] S.L. Arnab Dutta, Jianbo Hou, Mark H. Engelhard, John A. S. Roberts, Wendy J. Shaw, Journal of American Chemical Society, 135 (2013) 18490-18496.
[28] R.J.A. Nilusha Priyadarshani Boralugodage, Arnab Dutta, Garry W. Buchko, Wendy J. Shaw, Catalysis Science & Technology, 7 (2017) 1108-1121.
[29] M.S. Yamauchi Kosei, Ken Sakai, Dalton Transactions, 40 (2011) 12447-12449.
[30] M.C. R. H. Herber, M. J. Coyer, B. Bilash, A. Sahiner Inorganic Chemistry, 33 (1994) 2422-2426.
[31] C. Gourlaouen, D. Chantal, Dalton Transactions, 43 (2014,) 17806-17819.
[32] L.M.H. William B. Connick, Richard E. Marsh, Harry B. Gray, Inorganic Chemistry, 35 (1996) 6261-6265.
[33] F.E. Appoh, H.B. Kraatz, Journal of applied polymer science, 111 (2009) 709-723.
[34] D. Kim, J.-L. Brédas, Journal of the American Chemical Society, 131 (2009) 11371-11380.
[35] Y. Li, L. Chen, Y. Ai, E.Y.-H. Hong, A.K.-W. Chan, V.W.-W. Yam, Journal of the American Chemical Society, (2017).
[36] Y.g. Sun, Y. Guo, D. Sun, M.c. Zhu, F. Ding, Y.n. Liu, E.j. Gao, S.j. Wang, G. Xiong, I. Dragutan, European Journal of Inorganic Chemistry, 2014 (2014) 5741-5751.
[37] D.L. Iqbal Bhugun, Jean-Michel Save´ant, Journal of the American Chemical Society, 118 (1996) 39823983.
[38] M. Kobayashi, S. Masaoka, K. Sakai, Angewandte Chemie International Edition, 51 (2012) 7431-7434.

Highlights:

- Four new platinum-*L*-glutamic acid dendrimer conjugates have been synthesized
- The dendrimer contains dichlorobipyridineplatinum(II) complex at the dendrimer core
- The conjugates characterization have been performed by spectroscopic techniques
- The dendrimers pose a substantial electronic and steric impact on the platinum core
- The dendrimer size effects the reduction rate of protons to molecular hydrogen

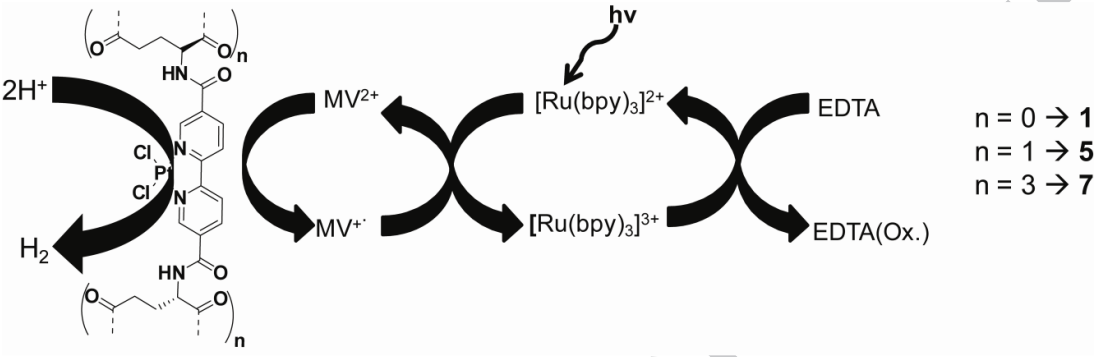

A series of platinum-glutamic amino acid conjugates have been synthesized. The identities of the bioconjugates have been confirmed by ^{1}H-, ^{13}C NMR, UV-vis and IR spectroscopy as well as mass (MS) spectrometry. The platinum bioconjugates have shown different reactivity towards the visible-light induced water splitting to generate hydrogen gas. The catalyst structure-activity relationship is disuccsed